ELSEVIER

Mechanisms of Development 107 (2001) 119–131

www.elsevier.com/locate/modo

The Alzheimer-related gene *presenilin-1* facilitates *sonic hedgehog* expression in *Xenopus* primary neurogenesis

Alejandra R. Paganelli[a], Oscar H. Ocaña[a], María I. Prat[b], Paula G. Franco[a], Silvia L. López[a], Laura Morelli[b], Ana M. Adamo[b], Martín M. Riccomagno[a], Etsuro Matsubara[c], Mikio Shoji[c], José L. Affranchino[d], Eduardo M. Castaño[b], Andrés E. Carrasco[a,*]

[a]*Laboratorio de Embriología Molecular, Instituto de Biología Celular y Neurociencias, Facultad de Medicina, Universidad de Buenos Aires, Paraguay 2155, 3° piso (1121), Buenos Aires, Argentina*

[b]*Instituto de Química y Fisicoquímica Biológicas (IQUIFIB) and Departamento de Química Biológica, Facultad de Farmacia y Bioquímica, Universidad de Buenos Aires, Junín 956 (1113), Buenos Aires, Argentina*

[c]*Department of Neurology, Gunma University School of Medicine, Gunma, Japan*

[d]*Centro de Virología Animal (CEVAN-CONICET), Buenos Aires, Argentina*

Received 26 January 2001; received in revised form 14 May 2001; accepted 6 June 2001

Abstract

We analyzed the influence of *presenilins* on the genetic cascades that control neuronal differentiation in *Xenopus* embryos. Resembling *sonic hedgehog* (*shh*) overexpression, *presenilin* mRNA injection reduced the number of *N-tubulin*$^+$ primary neurons and modulated *Gli3* and *Zic2* according to their roles in activating and repressing primary neurogenesis, respectively. *Presenilin* increased *shh* expression within its normal domain, mainly in the floor plate, whereas an antisense *X-presenilin-α* morpholino oligonucleotide reduced *shh* expression. Both *shh* and *presenilin* promoted cell proliferation and apoptosis, but the effects of *shh* were widely distributed, while those resulting from *presenilin* injection coincided with the range of *shh* signaling. We suggest that *presenilin* may modulate primary neurogenesis, proliferation, and apoptosis in the neural plate, through the enhancement of *shh* signaling.

Keywords: *Sonic hedgehog*; *Presenilin*; Primary neurogenesis; Proliferation; Apoptosis; Morpholino oligonucleotide; *Xenopus laevis*

1. Introduction

The most common forms of familial Alzheimer's disease (AD) are associated to mutations in the *amyloid precursor protein* (*APP*), *presenilin-1* (*Ps1*), and *presenilin-2* (*Ps2*) genes (Selkoe, 1999). *APP* is cleaved by a series of secretases, and a critical event in the pathogenesis of AD occurs when an altered γ-secretase activity overproduces the 42 amino acid isoform of the *amyloid-β* peptide, which accumulates in the cerebral cortex as an early and invariant marker of the disease. Deletion of *Ps1* greatly reduces γ-secretase activity in mice (De Strooper et al., 1998), and recent evidences indicated that *presenilins* may contain the active site (Li et al., 2000).

Presenilins are polytopic membrane proteins located in the endoplasmic reticulum, Golgi complex, plasma membrane, and nuclear envelope (Cook et al., 1996; Kovacs et al., 1996; Walter et al., 1996; De Strooper et al., 1997). *Ps1* and *Ps2* genes encode 46- and 55-kDa proteins, respectively, about 80% homologous, with eight transmembrane domains and a large hydrophilic loop facing to the cytoplasm (Mattson et al., 1998). They undergo endoproteolysis within the loop domain, and the resultant 30-kDa N-terminal and 20-kDa C-terminal fragments combine into stable 1:1 heterodimers that may constitute the biologically active form (Capell et al., 1998).

In addition to their role in *APP* proteolysis, *presenilins* have been proposed to modulate programmed cell death (PCD) (Deng et al., 1996; Kim et al., 1997; Loetscher et al., 1997; Roperch et al., 1998; Passer et al., 1999; Ye and Fortini, 1999), intracellular calcium homeostasis (Buxbaum et al., 1998; Stabler et al., 1999), the cell response to protein misfolding in the endoplasmic reticulum (Niwa et al., 1999), and the *Wnt/β-catenin* pathway (Murayama et al., 1998; Levesque et al., 1999; Nishimura et al., 1999). Most of these functions have been studied in cultured cells and remain to be tested in vivo to determine their functional relevance.

* Corresponding author. Tel.: +5411-4508-3675 ext. 18; fax: +5411-4962-5457.

E-mail address: rqcarras@mail.retina.ar (A.E. Carrasco).

0925-4773/01/$ - see front matter
PII: S0925-4773(01)00458-0

Apart from the involvement of mutant *presenilins* in the pathogenesis of AD, most of what we know about the physiological role of *presenilins* has derived from the analysis of null phenotypes in *Caenorhabditis elegans*, *Drosophila melanogaster*, and mice. The emerging picture shows that they are central to neuronal differentiation. Evidences include the loss of neural progenitor cells and neurons from brains of *Ps1* null mice (Shen et al., 1997), disorganization of the trunk ventral neural tube in mice lacking both *Ps1* and *Ps2* (Donoviel et al., 1999) and the neurogenic phenotypes in *Drosophila presenilin* mutants (Ye et al., 1999). This role for *presenilins* is supported by their high levels of expression during periods of neurogenesis and their predominant location in the adult central nervous system (Berezovska et al., 1997; Shen et al., 1997; Mattson et al., 1998). However, despite studies concerning their facilitation of *Notch* signaling (De Strooper et al., 1999; Song et al., 1999; Struhl and Greenwald, 1999; Handler et al., 2000), the ability of *presenilins* to regulate different steps of the genetic cascades involved in neuronal differentiation has not been extensively explored. Therefore, we decided to focus on this subject using the *Xenopus* primary neurogenesis cascade as a well-established model of neuronal differentiation.

Two *Xenopus* homologues of human *Ps1* and *Ps2* have been isolated. The encoded proteins, *X-Ps-α* and *X-Ps-β*, are 89.4 and 85.9% similar to *Ps1* and *Ps2*, respectively. Competitive reverse transcriptase-polymerase chain reaction (RT-PCR) revealed high levels of both transcripts in the oocyte, which decreased during early development, and zygotic expression became evident at tailbud stages (Tsujimura et al., 1997).

Amphibian neurogenesis comprises two distinct waves of differentiation. Primary neurogenesis produces a simple network that mediates swimming and escape reflexes in the early tadpole and secondary neurogenesis further generates neurons involved in more complex behaviors of the late tadpole. In *Xenopus*, the first wave results in three stripes expressing the terminal neuronal differentiation marker *N-tubulin* arranged at both sides of the neural plate, containing primary motor neurons, interneurons, and sensory neurons, separately (Chitnis et al., 1995). This process is early controlled by the balanced expression of prepattern genes. Amongst them are members of the *Gli* and *Zic* family of zinc finger transcription factors (Lee et al., 1997; Marine et al., 1997; Brewster et al., 1998; Nakata et al., 1998). Within the neural plate, *Gli3* is expressed in a graded fashion with highest levels in lateral regions and *Zic2* transcripts are arranged in stripes that alternate with those in which primary neuron formation takes place. While *Gli3* promotes neuronal differentiation, *Zic2* suppresses it. By exerting opposite functions, prepattern genes outline the sites where primary neuron formation will be permitted or excluded. Prepattern genes, in turn, regulate the more refined expression of proneural genes, a group of basic helix–loop–helix transcription factors such as *X-ngnr-1* and *Xash-3* (Zimmerman et al., 1993; Ma et al., 1996). Thus, proneural genes confer competence to neural cells of becoming differentiated neurons to more restricted domains. Within the proneural cluster, one cell is singled out to develop into a neuronal precursor, while the neighbors are prevented from doing so. This process of lateral inhibition is mediated by the neurogenic gene *Notch* and its membrane-bound ligand *Delta* (Chitnis et al., 1995). Proneural genes promote the expression of *Delta* in the selected cell (Ma et al., 1996). Then, *Delta* interacts with the receptor *Notch* on the surface of the neighboring cell. The receptor is cleaved to render the intracellular domain ($Notch^{ICD}$) that enters the nucleus and, in association with *CSL* intracellular transducers, activates the transcription of target genes of the *HES* family that, acting as transcriptional repressors, lead to suppression of neuronal fate (Wettstein et al., 1997; Bray, 1998).

Several evidences indicate that *presenilins* facilitate the *Notch* signaling pathway. From experiments with *Drosophila* mutants, it has been proposed that *presenilin* is required for activity and nuclear access of *Notch* (Struhl and Greenwald, 1999). Moreover, in vitro studies on mammalian cells have shown evidences that a *Ps1*-dependent γ-secretase-like activity mediates the intramembranous cleavage of the mature receptor to release $Notch^{ICD}$ (De Strooper et al., 1999). However, the *Notch* signaling pathway has been shown to remain partially activated even when the γ-secretase-like activity is blocked (Berezovska et al., 2000) and *Ps1* point mutations were able to separate *APP* proteolysis from *Notch* processing (Kulic et al., 2000). Other authors favor the idea that *presenilins* are required before $Notch^{ICD}$ release, during the maturation of the receptor (Ye et al., 1999), or in the secretory pathway (Ray et al., 1999).

Hedgehog proteins comprise a family of secreted molecules essential for patterning a variety of structures during animal embryogenesis (Lee et al., 1992; Riddle et al., 1993; Echelard et al., 1993; Krauss et al., 1993; Ekker et al., 1995). One of them, *sonic hedgehog* (*shh*), is expressed by the notochord and the floor plate in vertebrates. Either floor plate cells or ventral neurons can be induced in vitro by *Shh* protein in a concentration-dependent way (Roelink et al., 1995), indicating a role for *shh* signaling during patterning of the neural tube. It has been proposed that *HNF-3β*, a transcription factor of the winged-helix family, activates *shh* transcription in the notochord. Then, secreted *Shh* from the notochord activates *Gli1* in the midline of the neural plate. *Gli1*, in turn, switches on *HNF-3β* which, ultimately, activates *shh* expression in floor plate cells. Finally, *shh* signaling from the floor plate induces motor neurons in adjacent cells of the ventral neural tube (Lee et al., 1997).

We have previously found in *Xenopus* embryos that retinoid and *hedgehog* signaling modulated primary neurogenesis by counterbalancing the expression of prepattern genes with opposite functions. While *Xenopus shh* (*X-shh*) negatively regulated genes that promote the neurogenesis

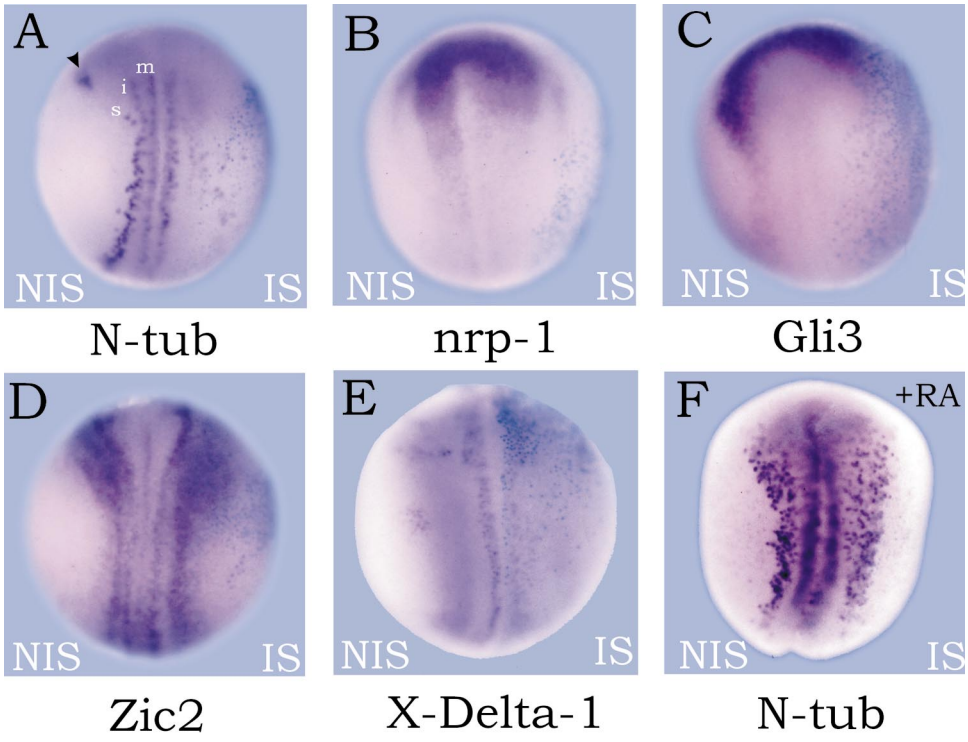

Fig. 1. Effects of *Ps1* mRNA injection on neural plate development. WMISH was performed at stage 14–15. All are dorsal views. Anterior is up. The injected side (IS) is demarcated by the pale blue X-gal staining. NIS, non-injected side. (A) Suppression of primary neurogenesis, revealed by *N-tubulin* (N-tub) (85%, $n = 40$). The trigeminal ganglion (arrowhead) was absent from the IS. m, i, and s, primary motorneurons, interneurons, and sensory neurons, respectively. (B) Expansion of the neural plate, revealed by *nrp-1* (100%, $n = 15$). (C) Reduction of *Gli3* expression (39%, $n = 41$). (D) Expansion of *Zic2* domains (73%, $n = 40$). (E) Reduction of *X-Delta-1* expression (80%, $n = 10$). (F) Rescue of primary neurogenesis by RA treatment in *Ps1*-injected embryos (100%, $n = 5$).

cascade, retinoids favored neurogenesis by repressing *X-shh* expression. Moreover, *shh* signaling may promote proliferation of neural precursors for later differentiation of secondary ventral neurons at the expense of primary neuron formation (Franco et al., 1999).

Here we show that the injection of human *Ps1* mRNA into *Xenopus* embryos produced changes along the primary neurogenesis cascade that closely resembled the effects of *X-shh* overexpression. Furthermore, both *Ps1* and *X-Ps-α* increased the amounts of *X-shh* transcripts, mainly in the floor plate, and an antisense morpholino oligonucleotide directed against the endogenous *X-Ps-α* mRNA reduced *X-shh* expression. In addition, while *X-shh* overexpression produced a widespread induction of proliferation and apoptosis, *Ps1* only promoted these responses within domains of *shh* signaling. We propose that *presenilin* may modulate primary neurogenesis, proliferation, and apoptosis by facilitating *X-shh* expression.

2. Results

2.1. Ps1 disfavors primary neuron formation without impairing neural development

To investigate whether *Ps1* is able to modulate primary neurogenesis, we examined the effects of unilateral *Ps1* injection on the pattern of *N-tubulin* at neurula stage. The injected side showed a down-regulation of *N-tubulin* predominantly in the intermediate and sensory stripes and in the trigeminal ganglion (Fig. 1A). Several embryos (65%, $n = 40$) revealed a ventral displacement of lateral neurons, perhaps because of an expansion of the neural plate. Therefore, we analyzed the expression of the general neural marker *nrp-1* (Knetch et al., 1995) and found that the *nrp-1* domain was expanded on the injected side (Fig. 1B). We conclude that *Ps1* can suppress primary neurogenesis, but this effect is not due to the inhibition of neural development.

2.2. Ps1 down-regulates Gli3 and promotes Zic2 expression

To analyze which steps of the neurogenesis cascade were modified by *Ps1* injection, we examined the distribution of transcripts corresponding to prepattern genes with opposite functions like *Gli3* and *Zic2* (Brewster et al., 1998). *Ps1*-injected embryos showed a down-regulation of *Gli3* (Fig. 1C). Conversely, *Zic2* expression was clearly expanded (Fig. 1D). Taken together, these results suggest that *Ps1* reduced primary neuron formation by controlling the balance of prepattern genes with antagonistic actions: while promoting the expression of the negative regulator

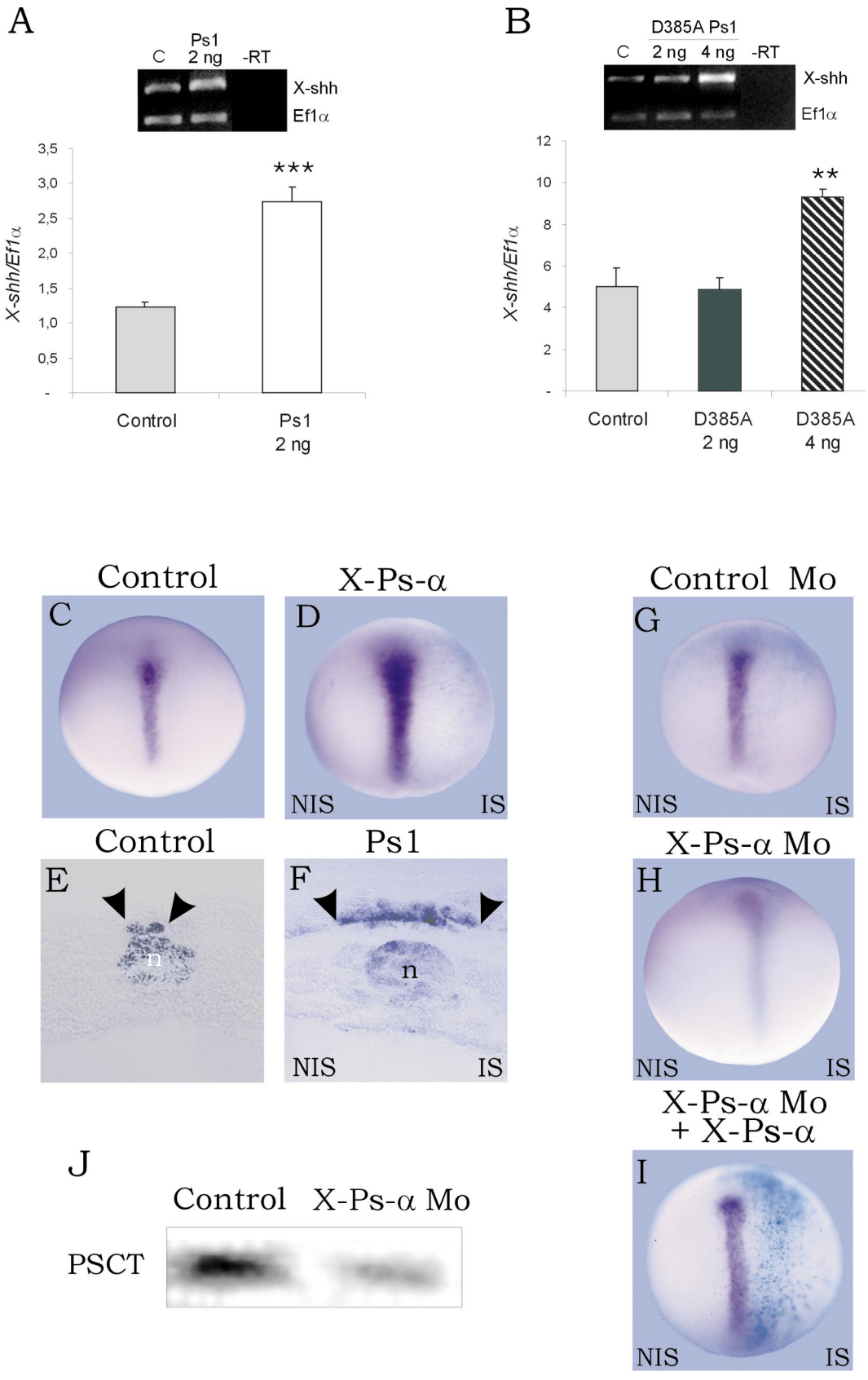
A
Ps1
C 2 ng -RT
X-shh
Ef1α
X-shh/Ef1α
***
Control
Ps1 2 ng
B
D385A Ps1
C 2 ng 4 ng -RT
X-shh
Ef1α
X-shh/Ef1α
**
Control
D385A 2 ng
D385A 4 ng
Control
X-Ps-α
Control Mo
C
D
G
NIS
IS
Control
Ps1
X-Ps-α Mo
E
F
H
n
NIS
IS
X-Ps-α Mo + X-Ps-α
J
Control X-Ps-α Mo
PSCT
I

Fig. 2

of neurogenesis *Zic2*, *Ps1* suppressed the positive regulator *Gli3*.

2.3. Retinoic acid (RA) counteracts the effects of Ps1 on primary neuron differentiation

Retinoids have the ability to enhance primary neurogenesis at very early steps, by controlling events upstream of the prepattern genes *Gli3* and *Zic2* (Franco et al., 1999). Since *Ps1* abolished primary neurogenesis, at least by an opposite control over these prepattern genes, we wanted to analyze the hierarchy of this regulation. Therefore, we considered whether RA treatment could overcome the *Ps1*-induced suppression of primary neurons. Unilaterally *Ps1*-injected embryos were treated with RA during gastrulation and the *N-tubulin* pattern was analyzed at neurula stage. We found that *N-tubulin* domains were clearly expanded despite *Ps1* injection (Fig. 1F). Therefore, RA rescues the inhibitory effect of *Ps1* on primary neuron development, arguing against a retinoid control on *Ps1* activity.

2.4. Ps1 impairs primary neurogenesis before lateral inhibition takes place

The impairment of primary neurogenesis by *Ps1* could be the consequence of enhancing lateral inhibition at the time of primary neurogenesis. However, we found that *X-Delta-1* domains were reduced after *Ps1* injection (Fig. 1E). Future primary neurons are the source of *X-Delta-1* (Chitnis et al., 1995) and *X-Delta-1* is under the positive control of *X-ngnr-1* (Ma et al., 1996). The down-regulation of *X-ngnr-1* in *Ps1*-injected embryos (data not shown) confirmed that a smaller amount of proneural precursors was produced, and this may account for the reduction of *X-Delta-1* expression. Therefore, instead of an enhancement of lateral inhibition, our results favor the hypothesis that *Ps1* interferes with the primary neurogenesis cascade before lateral inhibition takes place.

2.5. Presenilin increases X-shh expression and expands the floor plate domain

Because the injection of both *X-shh* (Franco et al., 1999) and *Ps1* mRNAs resulted in strikingly similar changes in the expression pattern of genes involved in primary neurogenesis, we examined whether *presenilin* and *shh* signaling were linked in the modulation of this process. Embryos injected with 2 ng of *Ps1* mRNA showed a significant increase of *X-shh* transcripts as revealed by quantitative RT-PCR (Fig. 2A). Whole-mount in situ hybridization demonstrated that this enhancement was not ectopic but instead, it only affected the normal domain of *X-shh* in the dorsal midline. This result was reproduced with *X-Ps-α* injections, indicating a functional conserved mechanism (Fig. 2D). Cross-sections revealed that amongst dorsal midline structures that normally express *X-shh*, *presenilin* injection selectively expanded the floor plate domain (compare Fig. 2E,F).

A loss-of-function approach with antisense morpholino oligos was recently shown to specifically prevent *β-catenin* activity in *Xenopus* embryos (Heasman et al., 2000). In order to block the endogenous *X-Ps-α* transcript an antisense morpholino (*X-Ps-α Mo*) was designed complementary to the 5′ UTR region of *X-Ps-α* mRNA, excluding sequences of the open reading frame (ORF). Since the reintroduction of synthetic target mRNA is a rigorous test of specificity only if the rescuing mRNA lacks the target region of the antisense morpholino (Heasman et al., 2000), the synthetic *X-Ps-α* mRNA fulfills this requirement, because the 5′ UTR was replaced by globin flanking sequences from the pCDG1 vector. While *X-Ps-α Mo* substantially reduced *X-shh* expression (Fig. 2H), the co-injection with *X-Ps-α* mRNA specifically reverted the phenotype (Fig. 2I); in addition, the injection of a standard negative control morpholino did not change *shh* expression (Fig. 2G). To further study the effect of *X-Ps-α Mo* on the expression of X-PS-α, we analyzed neural plate explants extracts by western blot using anti-PSCT, against the 39-residue carboxyl-terminus of human PS1 that shares complete identity to *X-Ps-α* corresponding sequence (Tsujimura et al., 1997). Anti-PSCT recognized an 18–20-kDa component, consistent with a carboxyl-terminal fragment (CTF) generated by the normal endoproteolysis of *X-Ps-α* and *β*, as described for presenilins in all studied species. This 18–20-kDa band was not detected when preimmune serum was used as a control. Densitometric analysis of western blots revealed significant reduction of X-PS-CTF immunoreactivity to 45% in *X-Ps-α Mo*-injected embryos

Fig. 2. *Presenilin* modulates *X-shh* expression. (A, B) Quantitative RT-PCR analysis of *X-shh* transcripts at stage 14–15. After *Ps1* mRNA bilateral injection, *Ps1* increased 122% the *X-shh/Ef1α* ratio ($P < 0.001$, $n = 3$) (A). Bilateral delivery of 2 ng of the mutant *D385A Ps1* mRNA did not significantly increase the *X-shh/Ef1α* ratio. However, delivery of 4 ng of the mutant *Ps1* mRNA increased 85% the *X-shh/Ef1α* ratio ($P < 0.01$, $n = 2$) (B). The constitutively expressed *Ef1α* transcript was used for normalizing results. Expression levels were compared using the *t*-test; SEMs are indicated by error bars; *n*, number of independent experiments, each consisting of RNA samples from ten control or injected embryos that were reverse transcribed and then subjected to quantitative PCR analysis by quadruplicate. On the top of each panel is shown the corresponding ethidium bromide-stained agarose gel of one representative determination. C, control embryos. Minus RT (−RT), PCR amplification without reverse transcriptase. (C–I) WMISH for *X-shh* showing that *presenilin* is able to modulate *X-shh* expression. The pale blue staining indicates the location of the *nucβ-gal* tracer. IS, injected side. NIS, non-injected side. Dorsal views of control (C), *X-Ps-α*- (D), standard control morpholino oligo- (control Mo) (G), *X-Ps-α Mo*- (H), and *X-Ps-α Mo* + *X-Ps-α*- (I) injected embryos, stage 13–14. Cross-sections of control (E) and *Ps1*-injected (F) embryos, stage 14. Compare arrowheads between (E, F), showing an expanded distribution of *X-shh* transcripts in the floor plate domain. The notochord (n) was unaffected. (J) Western blots of neural plate extracts with anti-PSCT. An 18–20-kDa immunoreactive band consistent with X-PS CTF endoproteolytic product is reduced in *X-Ps-α Mo*-injected embryos.

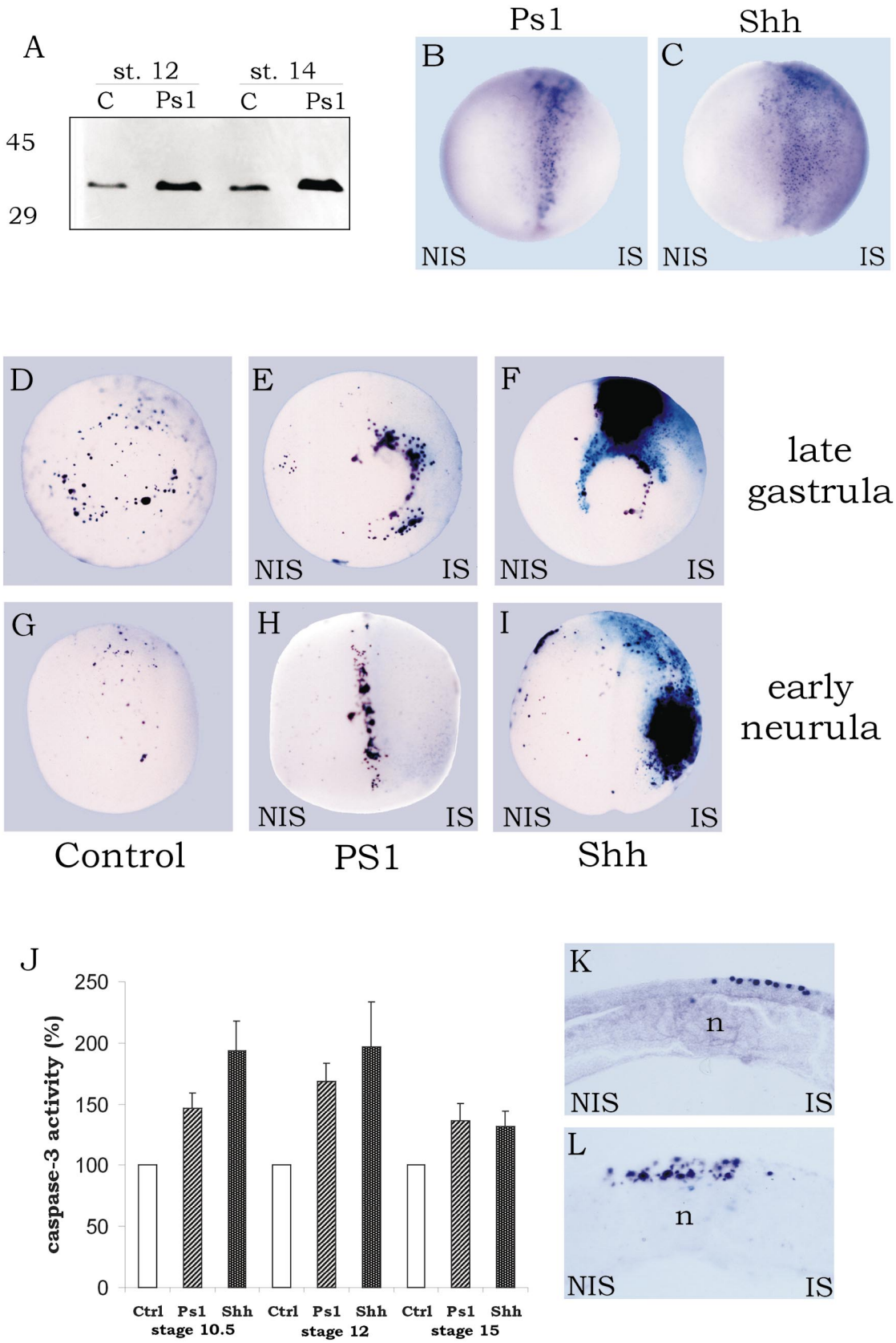
A
st. 12
st. 14
C
Ps1
C
Ps1
45
29
Ps1
Shh
B
C
NIS
IS
NIS
IS
D
E
F
NIS
IS
NIS
IS
late gastrula
G
H
I
NIS
IS
NIS
IS
early neurula
Control
PS1
Shh
J
caspase-3 activity (%)
250
200
150
100
50
0
Ctrl Ps1 Shh Ctrl Ps1 Shh Ctrl Ps1 Shh
stage 10.5
stage 12
stage 15
K
n
NIS
IS
L
n
NIS
IS

Fig. 3

as compared to controls (Fig. 2J). Since both *Xenopus* presenilins share 80% homology within their carboxyl-terminal sequence, the remaining signal in *X-Ps-α Mo*-injected embryos could be explained by the presence of *X-Ps-β* whose levels should be unaffected by *X-Ps-α Mo* injection. These results further support a positive control mechanism for *shh* expression by *presenilin*.

2.6. Ps1-enhancement of X-shh expression may not be mediated by γ-secretase activity

It has been described for *Ps1* that the substitution of the transmembrane aspartate residues 257 and 385 by alanine in either position substantially reduces γ-secretase activity on *APP* processing. In addition, either mutant appears to act as dominant negative with respect to endogenous *Ps1* (Wolfe et al., 1999). They preclude the entry of endogenous *presenilins* into a functional mature high molecular complex (Yu et al., 2000). Consequently, we considered whether these residues were essential for increasing *X-shh* transcripts, and we chose the *D385A Ps1* mutant for this purpose. First, we injected 2 ng of *D385A Ps1* mRNA, but quantitative RT-PCR did not reveal significant differences of *X-shh* levels between injected and control embryos (Fig. 2B). Since we did not perceive a dominant negative effect, we considered the possibility that the delivered amount of mutant mRNA was not sufficient to reduce *X-shh* expression. However, when 4 ng of *D385A Ps1* mRNA were injected, we observed a significant increase of *X-shh* transcripts (1.7-fold compared to control embryos; Fig. 2B). It is noteworthy that we had to inject twice the amount of mutant in relation to wild type *Ps1* mRNA to obtain a similar increase of *X-shh* transcripts (1.7- vs. 2.4-fold increase for mutant and wild type *Ps1*, respectively; compare Fig. 2A,B). Therefore, Asp 385 does not seem to be essential for modulating *X-shh* expression, although its substitution reduces the efficiency of *Ps1* for exerting this activity. Hence, we presume that the γ-secretase activity proposed for *Ps1* is unlikely modulating *X-shh* signaling. Alternatively, *D385A Ps1* may retain residual γ-secretase activity in *Xenopus* embryos. However, this activity was not reported for this mutant in transfected cell lines (Wolfe et al., 1999).

2.7. Ps1 stimulates cell proliferation under the influence of endogenous shh

Nuclear Hoechst staining revealed a higher cell number within the *Ps1*-injected side (not shown), therefore we considered the possibility that *Ps1* was inducing cell proliferation. Thus, we compared the expression of proliferating cell nuclear antigen (PCNA; Waseem and Lane, 1990) between control and *Ps1*-injected embryos. Western blot analysis of the detergent-soluble fraction revealed that at gastrulation and neurulation, PCNA levels were significantly higher after *Ps1* injection (Fig. 3A). This result was confirmed by densitometry of blots from two independent experiments. At gastrulation and neurulation PCNA levels in *Ps1*-injected embryos were four-fold and seven-fold higher, respectively, than in sibling controls. This result clearly demonstrates that *Ps1* has the ability to promote cell proliferation. Likewise, we have previously reported that *X-shh*-injected embryos had higher cell amounts on the injected side, leading us to propose a proliferative role for *X-shh* in the neural ectoderm (Franco et al., 1999). In order to verify this and to compare the distribution of proliferative cells after *Ps1* and *X-shh* mRNA injection, we performed whole-mount inmunolocalization of PCNA at neurula stage in unilaterally injected embryos. Both molecules produced a remarkable induction of proliferation on the injected side (Fig. 3B,C). It was significant to find out that while *X-shh* promoted proliferation all over the injected side, *Ps1* did it only within and around the dorsal midline (Fig. 3B,K), where *shh* signaling is normally operating. These results suggest that the effect of *Ps1* on proliferation may be mediated by the increase of *X-shh* expression in the floor plate.

2.8. Ps1 stimulates programmed cell death in domains of shh signaling

An involvement of *presenilins* in regulation of apoptosis has been suggested by previous investigations in various cell culture systems (see Section 1). Besides *Ps1* ability to promote proliferation, it was conceivable that a decrease of PCD also contributed to raise the cell number after *Ps1* injection. Since *Ps1* modulation of neural patterning and proliferation may be mediated by *shh* signaling, we inves-

Fig. 3. Effects of *presenilin* and *X-shh* injection on proliferation and programmed cell death. (A) Western blot of PCNA at stage 12 (st. 12, gastrula) and stage 14 (st. 14, neurula). C, controls; *Ps1*, embryos bilaterally injected with *Ps1* mRNA. One embryo equivalent was loaded per lane. Identical results were obtained from two independent experiments. On the left, molecular mass markers, in kDa. (B, C) Whole-mount inmunohistochemistry for PCNA after unilateral *Ps1* (B) or *X-shh* (C) injection. Dorsal views of stage 14 embryos are shown; anterior is up. IS, injected side. NIS, non-injected side. (D–J) *Ps1* and *X-shh* mRNA injection increased apoptosis. (D–I) Whole-mount TUNEL determination. Control embryos (D, G), embryos unilaterally injected with *Ps1* (E, H) or *X-shh* mRNA (F, I). All are dorsal views. Anterior is up. The injected side (IS) is demarcated by the pale blue X-gal staining. NIS, non-injected side. (D–F) Stage 12 embryos. (G–I) Stage 15 embryos. (J) *Caspase-3* activity determination. Embryos bilaterally injected with *Ps1* or *X-shh* mRNA show an increased *caspase-3* activity at stage 10.5 and at stage 12 (69% for *Ps1*, $n = 3$; 97% for *X-shh*, $n = 3$) when compared to controls (Ctrl, $n = 4$). *Caspase-3* activity declines at neurula stages (stage 15). Values are expressed as percentage of the activity from control extracts; SEMs are indicated by error bars; *n* indicates the number of independent *caspase-3* determinations, each consisting of extracts from 30 embryos. The observation that at neurulation TUNEL staining revealed strong signal while *caspase-3* activity declined is consistent with the fact that *caspase-3* activation precedes DNA fragmentation during apoptosis (Liu et al., 1997). (K) Cross-section of the embryo shown in (B). (L) Cross-section of the embryo shown in (H). n, notochord.

tigated whether *Ps1* and *X-shh* can also affect the apoptotic pattern.

The apoptotic signaling pathway involves the activation of death-specific proteases known as caspases. One of them, caspase-3, is a critical mediator responsible for dismantling cellular proteins (Salvesen and Dixit, 1997). As a quantitative measure of apoptosis, we determined caspase-3 activity at different stages in crude extracts from embryos injected with *Ps1* or *X-shh* mRNA. Both molecules produced a significant increase of caspase-3 activity, stronger at gastrulation (stages 10.5 and 12) than at neurulation (stage 15) (Fig. 3J). Therefore, we decided to compare the spatial distribution of apoptotic nuclei undergoing DNA fragmentation after *Ps1* and *X-shh* injection. Whole-mount TUNEL revealed that at stage 12 apoptotic cells are normally dispersed around the blastopore (Fig. 3D), as previously shown (Hensey and Gautier, 1998). While unilateral injection of *Ps1* enhanced apoptosis in a restricted region on the blastopore lip (Fig. 3E), *X-shh* produced a widespread and strong induction of apoptotic cells all over the injected side (Fig. 3F). Such different behaviors were observed again at neurula stages. While some scattered apoptotic cells were evident at stage 15 on the neural plate of control embryos (Fig. 3G), as previously reported (Hensey and Gautier, 1998), *Ps1* injection resulted in a clear induction of apoptosis in a dorsal midline stripe (Fig. 3H,L) and *X-shh* injection produced a remarkable induction of apoptosis in large patches on the injected side (Fig. 3I). Because an inhibition of PCD does not account for the increase in cell number observed after *X-shh* and *Ps1* injection, the induction of apoptosis by these molecules may be the result of a mechanism that counterbalances their proliferative stimulus. It is noteworthy that resembling the effects on proliferation, *X-shh* was capable of inducing extensive cell death while *Ps1*-induced apoptosis restricted to the places of normal *shh* signaling. All these evidences further support the idea that *presenilin* may regulate different mechanisms that contribute to neural patterning by modulating *X-shh* expression.

3. Discussion

3.1. Presenilin modulates the balance of prepattern genes and favors the suppression of primary neurons

Several reports suggest that *presenilins* may participate in neuronal development. Evidences include their abundant expression during periods of neurogenesis (Berezovska et al., 1997; Shen et al., 1997; Mattson et al., 1998), the loss of neural progenitor cells and neurons from brains of mice lacking *Ps1* (Shen et al., 1997), and the neurogenic phenotypes in *Drosophila presenilin* loss-of-function mutants (Ye et al., 1999). Apart from other studies concerning *presenilin* facilitation of *Notch* signaling (De Strooper et al., 1999; Struhl and Greenwald, 1999; Handler et al., 2000), here, within the frame of the *Xenopus* primary neurogenesis cascade, we explore the ability of *presenilin* to regulate different steps of the genetic pathways leading to neuronal differentiation.

We show that injection of *Ps1* mRNA in frog embryos produces a substantial suppression of *N-tubulin*$^+$ primary neurons. We propose that this effect is decided earlier in the cascade, as evidenced by the opposite changes in the expression of two prepattern genes with antagonistic actions. Hence, *Ps1* seems to control neurogenesis at least by increasing the expression of *Zic2*, a gene proposed to inhibit neuronal differentiation, and by reducing the expression of *Gli3*, an activator of neuron formation (Brewster et al., 1998), thus leading to a decrease of proneural domains, as confirmed by the disorganization of *X-ngnr-1* longitudinal stripes. This explains the reduction of *X-Delta-1* expression, because *X-Delta-1* is under the positive control of *X-ngnr-1* (Ma et al., 1996). Notwithstanding the reported observations that *Ps1* is a positive regulator of *Notch* processing (De Strooper et al., 1999; Struhl and Greenwald, 1999; Ye et al., 1999; Ray et al., 1999), our results indicate that the reduction of primary neurogenesis produced by *Ps1* was mainly due to the impairment of events that precede lateral inhibition in the genetic cascade and that this modulation occurs at some level upstream of prepattern genes.

3.2. Presenilin positively regulates X-shh expression within the domain of shh signaling

Our results indicate that *Ps1* can modulate the expression of prepattern genes in the same way as previously shown for *X-shh* overexpression (Franco et al., 1999), suggesting that both molecules share some regulatory pathway above this level in the primary neurogenesis cascade. After *Ps1* injection, we found a notorious increase of *X-shh* transcripts by quantitative RT-PCR. Yet, in situ hybridization revealed no ectopic sites of expression. Instead, both *Xenopus* and human *presenilin* expanded the distribution of *X-shh* transcripts in the floor plate domain, and blocking the endogenous *X-Ps-α* mRNA with an antisense morpholino oligo specifically reduced *X-shh* expression. Thus, we conclude that the *presenilin*-induced enhancement of *X-shh* expression cannot occur outside the domains of *shh* signaling. Taken together, our results indicate that *presenilin* may modulate the balance of prepattern genes by facilitating *X-shh* expression in the floor plate. Although retinoid signaling down-regulates *shh* expression (Franco et al., 1999), it is unlikely that this happens through the negative control of *presenilin* activity because RA treatment could rescue the inhibitory effect of *Ps1* on primary neuron development. Nevertheless, from our results we cannot discern whether *presenilins* and retinoids are part of two separate pathways with antagonistic functions converging on the control of *shh* signaling, or if *presenilins* are able to negatively modulate retinoid signaling, releasing *shh* from retinoid repression.

3.3. The enhancement of shh signaling by presenilin may be favoring proliferation and apoptosis against primary neuron differentiation

The suggestion of a proliferative role for *X-shh* in vivo at neural plate stages (Franco et al., 1999) gained support here, because *X-shh* overexpression promoted strong PCNA immunostaining all over the injected side. This is consistent with previous observations in mice that *shh* behaves as a mitogen for cultured perinatal neural retinal precursor cells (Jensen and Wallace, 1997), prevents neuronal differentiation, and induces proliferation of granule cerebellar cell precursors in vitro (Weschler-Reya and Scott, 1999) and also stimulates proliferation and blocks differentiation of spinal cord neural precursor cells at embryonic stages in vivo (Rowitch et al., 1999). In addition, here we show that *X-shh* stimulated PCD extensively, perhaps as a mechanism to counterbalance proliferation. We found that *Ps1* also favored proliferation and apoptosis, but unlike *X-shh* overexpression, both effects were restricted within and around the dorsal midline. Therefore, *X-shh* does not seem to require a located cofactor to modulate proliferation and apoptosis. In contrast, both processes can be regulated by *Ps1* only within the range of *X-shh* signaling. From these evidences we conclude that *Ps1* may interact with some factor(s) exclusively present within *shh* expression domains. The *Ps1*-induced proliferation pattern correlates in part with the expansion of the expression domain of *shh*, but also extends at some distance on the neural plate, consistent with the idea that *Ps1* enhances the production of a secreted molecule, perhaps *Shh* protein, which promotes proliferation in neural cells adjacent to the floor plate.

In spite of the suppression of primary neurogenesis and the simultaneous activation of cell proliferation in the neural plate, secondary neurogenesis was finally stimulated in the ventral neural tube after injection of either *X-shh* (Franco et al., 1999) or *Ps1* (not shown), as revealed by the ventral neural marker *Xsal-1* (Hollemann et al., 1996). This led us to presume that *shh* signaling could be withdrawing precursor cells from premature differentiation, holding their proliferative state, and reserving them for later waves of neuron formation. *Presenilin*, through the enhancement of *shh* signaling, may also contribute to this mechanism. This is consistent with the fact that mice lacking *Ps1* undergo premature differentiation of neural progenitor cells into post-mitotic neurons (Handler et al., 2000).

From all these evidences we propose that *presenilin* may promote proliferation and apoptosis and suppress primary neurogenesis by facilitating *shh* signaling.

3.4. How can presenilin modulate shh signaling?

The selective expansion of the *X-shh* expression domain in the floor plate resulting from *presenilin* injection is consistent with the observation that mice lacking both *presenilin* genes show complete absence of *shh* transcripts in the trunk ventral neural tube, but expression remains unaltered in the head and notochord (Donoviel et al., 1999). From these observations we infer that the failed development of *Nkx2.2*$^{+}$ motorneurons in the trunk of these mutants may be due to the absence of *shh* signaling from the floor plate. Because widespread expression of *presenilin* does not result in ectopic activation of *X-shh*, we propose that *presenilin* needs a cofactor spatially restricted to the dorsal midline of the embryo in order to facilitate *shh* expression in the floor plate. During the sequence of events following the *presenilin*-independent transcription of *shh* in the notochord until the activation of *shh* in the floor plate, *presenilin* activity could be interacting at any point. Much research has been focused to establish that *hedgehog* signaling can be regulated at several steps, during post-translational processing and trafficking of *Hedgehog* protein in sending cells, and during reception and signal transduction in the receiving cells (for review, see McMahon, 2000). In this scenario, *presenilins* could be facilitating any of these steps, either in the notochord (sending cells), or in the floor plate (receiving cells). Both hypotheses can equally explain why the absence of *presenilins* (Donoviel et al., 1999) as well as the injection of either *Ps1* or *X-Ps-α* mRNAs (this paper) can affect *shh* expression only in the ventral midline of the central nervous system. Several of the functional features proposed for *presenilins* may be involved in either of the indicated points of the *shh* signaling pathway. Amongst them, the γ-secretase activity may not be involved, because the substitution of Asp 385, which was shown to suppress such activity (Wolfe et al., 1999), did not abolish the ability of *Ps1* to increase *X-shh* transcripts. Nevertheless, it remains to be tested whether this mutant retains residual γ-secretase activity in *Xenopus* embryos. Other lines of research have proposed that *presenilins* play a role in trafficking and metabolism of membrane and secreted proteins in neurons (Naruse et al., 1998). Furthermore, numerous biochemical interactions have been described between *presenilins* and a variety of proteins, including members of the *β-catenin* family, cytoskeleton- and microtubule-associated proteins, calcium-binding proteins, G-proteins, and GTPases (Buxbaum et al., 1998; Murayama et al., 1998; Smine et al., 1998; Takashima et al., 1998; Zhang et al., 1998; Dumanchin et al., 1999; Levesque et al., 1999; Nishimura et al., 1999; Stabler et al., 1999; Noll et al., 2000).

Regardless of the mechanism underlying the interaction between *presenilins* and *shh* signaling, we propose from this body of evidence that the suppression of primary neurogenesis and the stimulation of proliferation and PCD by *shh* signaling from the floor plate may be facilitated by *presenilins*. Identifying the role of *presenilins* during *shh* signaling will provide clues to understand how these important molecules could interact. Finally, it will be interesting to explore whether *hedgehog* signaling is involved in the pathogenesis of familiar AD.

4. Experimental procedures

4.1. Embryo culture, RNA injections, treatments, and procedures

Albino *Xenopus laevis* embryos were obtained using standard methods (Stern and Holland, 1992) and staged according to Nieuwkoop and Faber (1994). At the desired stages, embryos were either fixed with MEMFA (Harland, 1991) for in situ hybridization analysis, whole-mount TUNEL and immunohistochemistry, or homogeneized for RNA extraction, western blot analysis, or *caspase-3* activity determination. The entire *X-Ps-α* ORF was obtained by RT-PCR from tailbuds RNA, inserted by Exo III mediated subcloning (Li and Evans, 1997) into the pCDG1 vector (Blumberg et al., 1998) that had been digested with Nco I and BamH I. The sequence was 100% identical to the published one (Tsujimura et al., 1997). Synthetic capped mRNAs for microinjection were obtained by in vitro transcription with the Megascript kit (Ambion), and were purified with the RNeasy mini kit (Qiagen). Two nanograms of human *Ps1*, *X-Ps-α*, or *X-shh* mRNAs or 2 and 4 ng of *D385A* human *Ps1* mRNA were microinjected per embryo. The *X-Ps-α* antisense oligodeoxynucleotide (*X-Ps-α Mo*) used was a 25-mer morpholino oligo (Gene Tools, LLC) with the base composition 5′-GTCAGCGGAATCTTCAGACACTTGG-3′, and was injected in doses of 5 or 10 ng per embryo. Delivery was done into the animal hemisphere of one or both blastomeres, at the two-cell stage. To test for the specificity of the phenotype, either 5 ng of a standard control morpholino oligo were injected (5′-CCTCTTACCTCAGTTACAATTTATA-3′) or a rescue experiment was carried out by co-injecting 5 ng of *X-Ps-α Mo* together with 1 or 2 ng of *X-Ps-α* mRNA. Injections always included 100 pg of *nuc-βgal* mRNA as tracer. Embryos were maintained in 6% Ficoll, 1× Barth-Hepes saline (BHS; Gurdon, 1976) until 1 h after injection, and then were cultured in 3% Ficoll, 0.1× BHS until sibling controls reached the desired stage. Treatments with 10 μM all-trans RA (Sigma) were performed in 0.1× BHS from stage 9–10 until stage 15. X-gal staining, preparation of digoxigenin-labeled antisense RNA probes, whole-mount in situ hybridization (WMISH) and histological sections in paraplast were performed as previously described (Franco et al., 1999). For TUNEL and PCNA processed embryos, 50-μm sections were taken in an Oxford Vibratome and mounted onto gelatin-coated slides as described by Hollemann et al. (1996).

4.2. Site-directed mutagenesis

Human wild type *Ps1* was used as template to introduce *D385A* by asymmetric PCR-based site-directed mutagenesis. The following primers were used in the first PCR: forward 5′-GAAGGATCCACGAGCCGCGGC-3′ and reverse 5′-AGAAAAGTGAAAGCTCCCAATCCAAG-3′. The PCR product was purified and used as forward primer in a second reaction with the reverse primer 5′-TCAGAATTCAGTTAATACAGAATTATT-3′. The resultant mutant was cloned into the vector pcDNA3 (Invitrogen), and the identity was confirmed by sequencing.

4.3. Quantitative RT-PCR

For each experiment, total RNA was isolated at stage 14–15 from ten embryos, using the SV Total RNA Isolation System (Promega). Two micrograms of total RNA were reverse transcribed with Superscript™ II RNase H⁻ Reverse Transcriptase (Gibco BRL). PCR was carried out with Taq DNA polymerase (Promega) in 50-μl reactions. Temperature cycles consisted of 94, 60, and 72°C steps, 30 s each, with an initial 5-min denaturation step at 94°C. Final extension was at 72°C, 5 min. Ten microliters of the reaction were analyzed on ethidium bromide-2% agarose gels. Experiments always included non-reverse transcribed RNA samples as negative controls. The number of cycles and the template input for PCR were determined empirically in each case, within the linear range of amplification. The forward (F) and reverse (R) primer sequences, the product sizes, and the number of cycles were as follows: *Ef1α*: F 5′-CAGATTGGTCCTGGATATGC-3′, R 5′-ACTGCCTTGATGACTCCTAG-3′, 268 bp, 25 cycles; *X-shh*: F 5′-ATCTCCGTGATGAACCAGGT-3′, R 5′-CAGACTTGAACGACCTGGTG-3′, 526 bp, 34 cycles. Each independent experiment was subjected to PCR analysis by quadruplicate. *X-shh* was normalized to the amount of the constitutively expressed *Ef1α* transcript. Measurements were done with Sigma Gel software.

4.4. Caspase-3 activity

Embryos were washed in PBS and homogeneized in 10 mM Tris–HCl, 10 mM $NaH_2PO_4/NaHPO_4$ pH 7.5, 130 mM NaCl, 1% Triton X-100, 10 mM NaPPi, with a glass Pyrex homogenizer. Homogenates were centrifuged for 10 min at 13 000 × *g* at 4°C. *Caspase-3* activity was determined in the supernatants with the PharMingen-Becton Dickinson *caspase-3* assay kit. Fluorescence was normalized against protein concentration.

4.5. Whole-mount TUNEL

Whole-mount TUNEL staining was based on the protocol of Hensey and Gautier (1997), with several modifications. Fixed embryos were shortly stored at 4°C in PBS. After rinsing in fresh PBS, they were treated for 15 min with 2.5 μg/ml proteinase K (Merck) in PTW (PBS containing 0.2% Tween 20) at room temperature, then refixed for 30 min with 4% formaldehyde in PBS and washed several times with PBS. Following 1 h preincubation with terminal deoxynucleotidyl transferase (TdT) buffer, reaction with 300 U/ml terminal TdT (GIBCO BRL) proceeded overnight at room temperature in the presence of 1 μM digoxigenin-dUTP (Boehringer Mannheim) and was stopped by treat-

ment for 2 h at 65°C in PBS containing 1 mM EDTA. Embryos were extensively washed in PBS, then for 15 min in PBT (PBS containing 2 mg/ml bovine serum albumin and 0.1% Triton X-100), and treated for 1 h with blocking buffer containing 2% Boehringer Mannheim blocking reagent in MAB (100 mM maleic acid, 150 mM NaCl, pH 7.5). After overnight incubation at 4°C with anti-digoxigenin antibody coupled to alkaline phosphatase (Boehringer Mannheim) diluted 1/2000 in blocking buffer, embryos were extensively washed in PBT at room temperature, followed by an overnight wash at 4°C in PBT. Following two short changes of alkaline phosphatase buffer (100 mM Tris–HCl pH 9.5, 50 mM $MgCl_2$, 100 mM NaCl, 0.1% Tween 20, 5 mM levamisol), staining was developed at 37°C in the same buffer containing 337 μg/ml nitro blue tetrazolium (NBT) and 175 μg/ml 5-bromo-4-chloro-3-indolyl phosphate (BCIP). After washing in methanol, embryos were rehydrated and viewed.

4.6. Sodium dodecyl sulfate-polyacrylamide gels (SDS-PAGE) and western blots

Embryos were homogenized in 50 mM Tris–HCl pH 8.0, 25% glycerol, 50 mM KCl, 2 mM DTT, 2 mM PMSF, 0.1 mM EDTA, 10 μg/ml aprotinin, and 10 μg/ml leupeptin, and centrifuged at 11 000 rpm at 4°C, 8 min. Pellets were resuspended in 150 mM NaCl, 10 mM Tris–HCl pH 7.4, 0.5% NP40, 5 mM EDTA, 2% SDS, 2 mM PMSF, 10 μg/ml leupeptin, 0.1 μg/ml pepstatin, sonicated on ice, and centrifuged as before. Supernatants were mixed with equal volumes of sample buffer containing 8% SDS and 0.1 M DTT, boiled for 3 min, and subjected to electrophoresis on 10% Tris–tricine SDS-PAGE. Proteins were transferred to PVDF membranes and probed with PCNA monoclonal antibody (Santa Cruz Biotechnology, Inc.). After incubation with horseradish peroxidase-labeled secondary antibody (Bio Rad), the reaction was visualized with ECL plus (Amersham-Pharmacia). Densitometry was performed with Gel Pro Analyzer software (Media Cybernetics).

To quantitate the expression of X-Ps-α protein, neural plate explants were solubilized in sample buffer containing 8% SDS. Five explants were loaded per lane in 10% Tris–tricine gels and blotted with anti-PSCT. Immunoreactive bands were developed as above and analyzed with a STORM 840 Imaging system (Molecular Dynamics).

4.7. Presenilin antibodies

Polyclonal antibodies were raised in rabbits using glutathione-*S*-transferase (GST) fused to amino acids 429–467 of human PS1. The antiserum (anti-PSCT) was sequentially purified using a BL21/GST lysate and the immunogen coupled to CNBr-activated sepharose (Pharmacia) as affinity columns, respectively. Specificity of anti-PSCT was tested against GST and fusion protein by western blot as described previously.

4.8. PCNA immunohistochemistry

Fixed embryos were washed twice in PBS and thrice in PBS containing 0.3% Triton X-100, for 15 min each, and left overnight at 4°C in blocking buffer. They were incubated for 5 h at room temperature with PCNA antibody diluted 1/50 in blocking buffer, washed twice at room temperature and overnight at 4°C with PTW, and thrice with PBS, for 10 min each. Then, they were left for 30 min in blocking buffer and incubated for 5 h at room temperature with anti-mouse antibody coupled to alkaline phosphatase (Promega) diluted 1/500 in blocking buffer. After washing twice for 15 min at room temperature and overnight at 4°C with PTW, color reaction was developed at 37°C with 337 μg/ml NBT and 175 μg/ml BCIP. Embryos were rinsed in distilled water, washed in methanol, and rehydrated for viewing.

Acknowledgements

We thank Dr Richard Harland for *nuc-βgal*, Igor Dawid for *N-tubulin*, Eric Bellefroid for *X-ngnr-1*, *nrp-1* and *X-Delta-1*; Ariel Ruiz i Altaba for *Zic2*, Tomas Pieler for *Gli3*, Reimer Stick for *Xsal-1*, Stephen Ekker for *X-shh* injection construct, Bruce Blumberg for critical reading of the manuscript and Sarah Daijogo from his laboratory, for PCR cloning of *X-Ps-α*, and Carmel Hensey and Jean Gautier for their TUNEL protocol. We are also grateful to Dr Steve Younkin for his agreement to use the human *presenilin-1* cDNA. We also wish to recognize Andrés Carrasco Jr. for helping with the artwork. A.R.P., L.M., S.L.L., A.M.A., J.L.A. and A.E.C. are from CONICET, Argentina. P.G.F. is supported by a fellowship from ANPCyT. M.I.P. is supported by a fellowship from FOMEC. This paper was supported by grants to A.E.C. from CONICET (PIP 0848/98), ANPCyT (BID802/OC-AR PICT 3410) and Beca Ramón Carrillo-Arturo Oñativia 2000 to L.M. and E.M.C., from ANPCyT (PICT98-05-04394) to E.M.C. from Beca Ramón Carrillo-Arturo Oñativia 2000 and to S.L.L. from CONICET (PEI 0322/98).

References

Berezovska, O., Xia, M., Page, K., Wasco, W., Tanzi, R., Hyman, B., 1997. Developmental regulation of *presenilin* mRNA expression parallels *notch* expression. J. Neuropathol. Exp. Neurol. 56, 40–44.

Berezovska, O., Jack, C., McLean, P., Aster, J., Hicks, C., Xia, W., Wolfe, M., Taylor Kimberly, W., Weinmaster, G., Selkoe, D., Hyman, B., 2000. Aspartate mutations in *presenilin* and γ-secretase inhibitors both impair *Notch1* proteolysis and nuclear translocation with relative preservation of *Notch1* signaling. J. Neurochem. 75, 583–593.

Blumberg, B., Kang, H., Bolado, J., Chen, H., Craig, A.G., Moreno, T.A., Umesono, K., Perlmann, T., De Robertis, E.M., Evans, R.M., 1998. *BXR*, an embryonic orphan nuclear receptor activated by a novel class of endogenous benzoate metabolites. Genes Dev. 12, 1269–1277.

Bray, S., 1998. A *Notch* affair. Cell 93, 499–503.

Brewster, R., Lee, J., Ruiz i Altaba, A., 1998. *Gli/Zic* factors pattern the

neural plate by defining domains of cell differentiation. Nature 393, 579–583.

Buxbaum, J., Choi, E., Luo, Y., Lilliehook, C., Crowley, A., Merriam, D., Wasco, W., 1998. *Calsenilin*: a calcium-binding protein that interacts with the *presenilins* and regulates the levels of a *presenilin* fragment. Nat. Med. 4, 1177–1181.

Capell, A., Grünberg, J., Pesold, B., Diehlmann, A., Citron, M., Nixon, R., Beyreuther, K., Selkoe, D., Haass, C., 1998. The proteolytic fragments of the Alzheimer's disease-associated *presenilin-1* form heterodimers and occur as a 100–150-kDa molecular mass complex. J. Biol. Chem. 273, 3205–3211.

Chitnis, A., Enrique, D., Lewis, J., Ish-Horowicz, D., Kintner, C., 1995. Primary neurogenesis in *Xenopus* embryos regulated by a homologue of the *Drosophila* neurogenic gene *Delta*. Nature 375, 761–766.

Cook, D., Sung, J., Golde, T., Felsenstein, K., Wojczyk, B., Tanzi, R., Trojanowski, J., Lee, V., Doms, R., 1996. Expression and analysis of *presenilin 1* in a human neuronal system: localization in cell bodies and dendrites. Proc. Natl Acad. Sci. USA 93, 9223–9228.

Deng, G., Pike, C., Cotman, C., 1996. Alzheimer-associated *presenilin-2* confers increased sensitivity to apoptosis in PC12 cells. FEBS Lett. 397, 50–54.

De Strooper, B., Beullens, M., Contreras, B., Levesque, L., Craessaerts, K., Cordell, B., Moechars, D., Bollen, M., Fraser, P., St. George-Hyslop, P., Van Leuven, F., 1997. Phosphorylation, subcellular localization, and membrane orientation of the Alzheimer's disease-associated *presenilins*. J. Biol. Chem. 272, 3590–3598.

De Strooper, B., Saftig, P., Craessaerts, K., Vanderstichele, H., Guhde, G., Annaert, W., Von Figura, K., Van Leuven, F., 1998. Deficiency of *presenilin-1* inhibits the normal cleavage of amyloid precursor protein. Nature 391, 387–390.

De Strooper, B., Annaert, W., Cupers, P., Saftig, P., Craessaerts, K., Mumm, J., Schroeter, E., Schrijvers, V., Wolfe, M., Ray, W., Goate, A., Kopan, R., 1999. A *presenilin-1*-dependent γ-secretase-like protease mediates release of *Notch* intracellular domain. Nature 398, 518–522.

Donoviel, D., Hadjantonakis, A., Ikeda, M., Zheng, H., Hyslop, P., Bernstein, A., 1999. Mice lacking both *presenilin* genes exhibit early embryonic patterning defects. Genes Dev. 13, 2801–2810.

Dumanchin, C., Czech, C., Campion, D., Cuif, M., Poyot, T., Martin, C., Charbonnier, F., Goud, B., Pradier, L., Frebourg, T., 1999. *Presenilins* interact with *Rab11*, a small GTPase involved in the regulation of vesicular transport. Hum. Mol. Genet. 8, 1263–1269.

Echelard, Y., Epstein, D., St-Jacques, B., Shen, L., Mohler, J., McMahon, J., McMahon, P., 1993. *Sonic hedgehog*, a member of a family of putative signaling molecules, is implicated in the regulation of CNS polarity. Cell 75, 1417–1430.

Ekker, S., McGrew, L., Lai, C.-J., Lee, J., Von Kessler, D., Moon, R., Beachy, P., 1995. Distinct expression and shared activities of members of the *hedgehog* gene family of *Xenopus laevis*. Development 121, 2337–2347.

Franco, P., Paganelli, A., López, S., Carrasco, A., 1999. Functional association of retinoic acid and *hedgehog* signaling in *Xenopus* primary neurogenesis. Development 126, 4257–4265.

Gurdon, J., 1976. Injected nuclei in frog oocytes: fate, enlargement, and chromatin dispersal. J. Embryol. Exp. Morphol. 36, 523–540.

Handler, M., Yang, X., Shen, J., 2000. *Presenilin-1* regulates neuronal differentiation during neurogenesis. Development 127, 2593–2606.

Harland, R., 1991. In situ hybridization: an improved whole mount method for *Xenopus* embryos. Methods Cell Biol. 36, 685–695.

Heasman, J., Kofron, M., Wylie, C., 2000. *β-catenin* signaling activity dissected in the early *Xenopus* embryo: a novel antisense approach. Dev. Biol. 222, 124–134.

Hensey, C., Gautier, J., 1997. A developmental timer that regulates apoptosis at the onset of gastrulation. Mech. Dev. 69, 183–195.

Hensey, C., Gautier, J., 1998. Programmed cell death during *Xenopus* development: a spatio-temporal analysis. Dev. Biol. 203, 36–48.

Hollemann, T., Schuh, R., Pieler, T., Stick, R., 1996. *Xenopus Xsal-1*, a vertebrate homolog of the region specific homeotic gene *spalt* of *Drosophila*. Mech. Dev. 55, 19–32.

Jensen, A., Wallace, V., 1997. Expression of *Sonic hedgehog* and its putative role as a precursor cell mitogen in the developing mouse retina. Development 124, 363–371.

Kim, T., Pettingell, W., Jung, Y., Kovacs, D., Tanzi, R., 1997. Alternative cleavage of Alzheimer-associated *presenilins* during apoptosis by a *caspase-3* family protease. Science 277, 373–376.

Knetch, A., Good, P., Dawid, I., Harland, R., 1995. Dorsal–ventral patterning and differentiation of *noggin*-induced neural tissue in the absence of mesoderm. Development 121, 1927–1936.

Kovacs, D., Fausett, H., Page, K., Kim, T., Moir, R., Merriam, D., Hollister, R., Hallmark, O., Mancini, R., Felsenstein, K., Hyman, B., Tanzi, R., Wasco, W., 1996. Alzheimer-associated *presenilins 1* and *2*: neuronal expression in brain and localization to intracellular membranes in mammalian cells. Nat. Med. 2, 224–229.

Krauss, S., Concordet, J., Ingham, P., 1993. A functionally conserved homologue of the *Drosophila* segment polarity gene *hh* is expressed in tissues with polarizing activity in zebrafish embryos. Cell 75, 1431–1444.

Kulic, L., Walter, J., Multhaup, G., Teplow, D., Baumeister, R., Romig, H., Capell, A., Steiner, H., Haass, C., 2000. Separation of *presenilin* function in *amyloid β*-peptide generation and endoproteolysis of *Notch*. Proc. Natl. Acad. Sci. USA 97, 5913–5918.

Lee, J., von Kessler, D., Parks, S., Beachy, P., 1992. Secretion and localized transcription suggest a role in positional signaling for products of the segmentation gene *hedgehog*. Cell 71, 33–50.

Lee, J., Platt, K., Censullo, P., Ruiz i Altaba, A., 1997. *Gli1* is a target of *sonic hedgehog* that induces ventral neural tube development. Development 124, 2537–2552.

Levesque, G., Yu, G., Nishimura, M., Zhang, D.M., Levesque, L., Yu, H., Xu, D., Liang, Y., Rogaeva, E., Ikeda, M., Duthie, M., Murgolo, N., Wang, L., VanderVere, P., Bayne, M.L., Strader, C.D., Rommens, J.M., Fraser, P.E., St. George-Hyslop, P., 1999. *Presenilins* interact with *armadillo* proteins including neural-specific *plakophilin*-related protein and *β-catenin*. J. Neurochem. 72, 999–1008.

Li, C., Evans, R.M., 1997. Ligation independent cloning irrespective of restriction site compatibility. Nucleic Acids Res. 25, 4165–4166.

Li, Y., Xu, M., Lai, M., Huang, Q., Castro, J., DiMuzio-Mower, J., Harrison, T., Lellis, C., Nadin, A., Neduvelil, J., Bruce Register, R., Sardana, M., Shearman, M., Smith, A., Shi, X., Yin, K., Shafer, J., Gardell, S., 2000. Photoactivated γ-secretase inhibitors directed to the active site covalently label *presenilin 1*. Nature 405, 689–694.

Liu, X., Zou, H., Slaughter, C., Wang, X., 1997. *DFF*, a heterodimeric protein that functions downstream of *caspase-3* to trigger DNA fragmentation during apoptosis. Cell 89, 175–184.

Loetscher, H., Deuchle, U., Brockhaus, M., Reinhardt, D., Nelboeck, P., Mous, J., Grunberg, J., Haass, C., Jacobsen, H., 1997. *Presenilins* are processed by caspase-type proteases. J. Biol. Chem. 272, 20655–20659.

Ma, Q., Kintner, C., Anderson, D., 1996. Identification of *neurogenin*, a vertebrate neuronal determination gene. Cell 87, 43–52.

Marine, J., Bellefroid, E., Pendeville, H., Martial, J., Pieler, T., 1997. A role for *Xenopus Gli*-type zinc finger proteins in the early embryonic patterning of mesoderm and neuroectoderm. Mech. Dev. 63, 211–225.

Mattson, M., Guo, Q., Furukawa, K., Pedersen, W., 1998. *Presenilins*, the endoplasmic reticulum, and neuronal apoptosis in Alzheimer's disease. J. Neurochem. 70, 1–14.

McMahon, A., 2000. More surprises in the *hedgehog* signaling pathway. Cell 100, 185–188.

Murayama, M., Tanaka, S., Palacino, J., Murayama, O., Honda, T., Sun, X., Yasutake, K., Nihonmatsu, N., Wolozin, B., Takashima, A., 1998. Direct association of *presenilin-1* with *β-catenin*. FEBS Lett. 433, 73–77.

Nakata, K., Nagai, T., Aruga, J., Mikoshiba, K., 1998. *Xenopus Zic* family and its role in neural and neural crest development. Mech. Dev. 75, 43–51.

Naruse, S., Thinakaran, G., Luo, J., Kusiak, J., Tomita, T., Iwatsubo, T.,

Qian, X., Ginty, D., Price, D., Borchelt, D., Wong, P., Sisodia, S., 1998. Effects of *PS1* deficiency on membrane protein trafficking in neurons. Neuron 21, 1213–1221.

Nieuwkoop, P., Faber, J., 1994. Normal Table of *Xenopus laevis* (Daudin), Garland Publishing, Inc, New York/London.

Nishimura, M., Yu, G., Levesque, G., Zhang, D.M., Ruel, L., Chen, F., Milman, P., Holmes, E., Liang, Y., Kawarai, T., Jo, E., Supala, A., Rogaeva, E., Xu, D.-M., Janus, C., Levesque, L., Bi, Q., Duthie, M., Rozmahel, R., Mattila, K., Lannfelt, L., Westaway, D., Mount, H.T.J., Woodgett, J., Fraser, P.E., St. George-Hyslop, P., 1999. *Presenilin* mutations associated with Alzheimer disease cause defective intracellular trafficking of β-*catenin*, a component of the *presenilin* protein complex. Nat. Med. 5, 164–169.

Niwa, M., Sidrauski, C., Kaufman, R., Walter, P., 1999. A role of *presenilin-1* in nuclear accumulation of *Ire 1* fragments and induction of the mammalian unfolded protein response. Cell 99, 691–702.

Noll, E., Medina, M., Hartley, D., Zhou, J., Perrimon, N., Kosik, K., 2000. *Presenilin* affects *Arm/*β-*catenin* localization and function in *Drosophila*. Dev. Biol. 15, 450–464.

Passer, B., Pellegrini, L., Vito, P., Ganjei, J., D'Adamio, L., 1999. Interaction of Alzheimer's *presenilin-1* and *presenilin-2* with *Bcl-X(L)*. A potential role in modulating the threshold of cell death. J. Biol. Chem. 274, 24007–24013.

Ray, W., Yao, M., Nowotny, P., Mumm, J., Zhang, W., Wu, J., Kopan, R., Goate, A., 1999. Evidence for a physical interaction between *presenilin* and *Notch*. Proc. Natl. Acad. Sci. USA 96, 3263–3268.

Riddle, R., Johnson, R., Laufer, E., Tabin, C., 1993. *Sonic hedgehog* mediates the polarizing activity of the ZPA. Cell 75, 1401–1416.

Roelink, H., Porter, J., Chiang, C., Tanabe, Y., Chang, D., Beachy, P., Jessell, T., 1995. Floor plate and motor neuron induction by different concentrations of the amino-terminal cleavage product of *Sonic hedgehog* autoproteolysis. Cell 81, 445–455.

Roperch, J., Alvaro, V., Prieur, S., Tuynder, M., Nemani, M., Lethrosne, F., Piouffre, L., Gendron, M., Israeli, D., Dausset, J., Oren, M., Amson, R., Telerman, A., 1998. Inhibition of *presenilin 1* expression is promoted by *p53* and *p21waf-1* and results in apoptosis and tumor supression. Nat. Med. 4, 835–838.

Rowitch, D., St.-Jacques, B., Lee, S., Flax, J., Snyder, E., McMahon, A., 1999. *Sonic hedgehog* regulates proliferation and inhibits differentiation of CNS precursor cells. J. Neurosci. 19, 8954–8965.

Salvesen, G., Dixit, V., 1997. Caspases: intracellular signaling by proteolysis. Cell 91, 443–446.

Selkoe, D., 1999. Translating cell biology into therapeutic advances in Alzheimer's disease. Nature 399 (Suppl.), A23–A31.

Shen, J., Bronson, R., Chen, D., Xia, W., Selkoe, D., Tonegawa, S., 1997. Skeletal and CNS defects in *presenilin-1*-deficient mice. Cell 89, 629–639.

Smine, A., Xu, X., Nishiyama, K., Katada, T., Gambetti, P., Yadab, S., Wu, X., Shi, Y., Yasuhara, S., Homburger, V., Okamoto, T., 1998. Regulation of brain G-protein go by Alzheimer's disease gene *presenilin-1*. J. Biol. Chem. 273, 16281–16288.

Song, W., Nadeau, P., Yuan, M., Yang, X., Shen, J., Yankner, B., 1999. Proteolytic release and nuclear translocation of *Notch-1* are induced by *presenilin-1* and impaired by pathogenic *presenilin-1* mutations. Proc. Natl. Acad. Sci. USA 96, 6959–6963.

Stabler, S., Ostrowski, L., Janicki, S., Monteiro, M., 1999. A myristoylated calcium-binding protein that preferentially interacts with the Alzheimer's disease *presenilin 2* protein. J. Cell Biol. 145, 1277–1292.

Stern, C., Holland, P., 1992. Essential Developmental Biology. A Practical Approach, IRL Press, Oxford.

Struhl, G., Greenwald, I., 1999. *Presenilin* is required for activity and nuclear access of *Notch* in *Drosophila*. Nature 398, 522–525.

Takashima, A., Murayama, M., Murayama, O., Kohno, T., Honda, T., Yasutake, K., Nihonmatsu, N., Mercken, M., Yamaguchi, H., Sugihara, S., Wolozin, B., 1998. *Presenilin 1* associates with *glycogen synthase kinase-3*β and its substrate *tau*. Proc. Natl. Acad. Sci. USA 95, 9637–9641.

Tsujimura, A., Yasojima, K., Hashimoto-Gotoh, T., 1997. Cloning of *Xenopus presenilin-*α and β cDNAs and their differential expression in oogenesis and embryogenesis. Biochem. Biophys. Res. Commun. 231, 392–396.

Walter, J., Capell, A., Grünberg, J., Pesold, B., Schindzielorz, A., Prior, R., Podlisny, M., Fraser, P., Hyslop, P., Selkoe, D., Haass, C., 1996. The Alzheimer's disease-associated *presenilins* are differentially phosphorylated proteins located predominantly within the endoplasmic reticulum. Mol. Med. 2, 673–691.

Waseem, N., Lane, D., 1990. Monoclonal antibody analysis of the proliferating cell nuclear antigen (PCNA). Structural conservation and the detection of a nucleolar form. J. Cell Sci. 96, 126–129.

Weschler-Reya, R., Scott, M., 1999. Control of neuronal precursor proliferation in the cerebellum by *Sonic hedgehog*. Neuron 22, 103–114.

Wettstein, D., Turner, D., Kintner, C., 1997. The *Xenopus* homolog of *Drosophila Suppressor of Hairless* mediates *Notch* signaling during primary neurogenesis. Development 124, 693–702.

Wolfe, M., Xia, W., Ostaszewski, B., Diehl, T., Kimberly, T., Selkoe, D., 1999. Two transmembrane aspartates in *presenilin-1* required for *presenilin* endoproteolysis and γ-secretase activity. Nature 398, 513–517.

Ye, Y., Fortini, M., 1999. Apoptotic activities of wild-type and Alzheimer's disease-related mutant *presenilins* in *Drosophila melanogaster*. J. Cell Biol. 146, 1351–1364.

Ye, Y., Lukinova, N., Fortini, M., 1999. Neurogenic phenotypes and altered *Notch* processing in *Drosophila presenilin* mutants. Nature 398, 525–529.

Yu, G., Chen, F., Nishimura, M., Steiner, H., Tandon, A., Kawarai, T., Arawaka, S., Supala, A., Song, Y., Rogaeva, E., Holmes, E., Zhang, D., Milman, P., Fraser, P., Haass, C., George-Hyslop, P., 2000. Mutation of conserved aspartates affects maturation of both aspartate mutant and endogenous *presenilin 1* and *presenilin 2* complexes. J. Biol. Chem. 275, 27348–27353.

Zhang, W., Han, S., McKeel, D., Goate, A., Wu, J., 1998. Interaction of *presenilins* with the *filamin* family of actin-binding proteins. J. Neurosci. 18, 914–922.

Zimmerman, K., Shih, J., Bars, J., Collazo, A., Anderson, D.J., 1993. *XASH-3*, a novel *Xenopus achaete-scute* homolog, provides an early marker of planar neural induction and position along the mediolateral axis of the neural plate. Development 119, 221–232.